OPEN

Light: Science & Applications (2015) 4, e280; doi:10.1038/lsa.2015.53

www.nature.com/lsa

ORIGINAL ARTICLE

Ultrafast photonic PCR

Jun Ho Son[1,2], Byungrae Cho[1,2], SoonGweon Hong[1,2], Sang Hun Lee[1,2], Ori Hoxha[1], Amanda J Haack[1] and Luke P Lee[1,2,3,4]

Nucleic acid amplification and quantification *via* polymerase chain reaction (PCR) is one of the most sensitive and powerful tools for clinical laboratories, precision medicine, personalized medicine, agricultural science, forensic science and environmental science. Ultrafast multiplex PCR, characterized by low power consumption, compact size and simple operation, is ideal for timely diagnosis at the point-of-care (POC). Although several fast/ultrafast PCR methods have been proposed, the use of a simple and robust PCR thermal cycler remains challenging for POC testing. Here, we present an ultrafast photonic PCR method using plasmonic photothermal light-to-heat conversion *via* photon–electron–phonon coupling. We demonstrate an efficient photonic heat converter using a thin gold (Au) film due to its plasmon-assisted high optical absorption (approximately 65% at 450 nm, the peak wavelength of heat source light-emitting diodes (LEDs)). The plasmon-excited Au film is capable of rapidly heating the surrounding solution to over 150 °C within 3 min. Using this method, ultrafast thermal cycling (30 cycles; heating and cooling rate of 12.79±0.93 °C s^{-1} and 6.6±0.29 °C s^{-1}, respectively) from 55 °C (temperature of annealing) to 95 °C (temperature of denaturation) is accomplished within 5 min. Using photonic PCR thermal cycles, we demonstrate here successful nucleic acid (λ-DNA) amplification. Our simple, robust and low cost approach to ultrafast PCR using an efficient photonic-based heating procedure could be generally integrated into a variety of devices or procedures, including on-chip thermal lysis and heating for isothermal amplifications.
Light: Science & Applications (2015) **4,** e280; doi:10.1038/lsa.2015.53; published online 31 July 2015

Keywords: genomics; light-emitting diodes (LEDs); molecular diagnostics; personalized medicine; plasmonics; point-of-care (POC) diagnostics; polymerase chain reaction (PCR)

INTRODUCTION

After its initial invention in 1983 by Kary Mullis, polymerase chain reaction (PCR) has become an essential technique in the fields of clinical laboratories, agricultural science, environmental science, and forensic science.[1–8] PCR requires thermal cycling, or repeated temperature changes between two or three discrete temperatures to amplify specific nucleic acid target sequences. To achieve such thermal cycling, conventional bench-top thermal cyclers generally use a metal heating block powered by Peltier elements. Whereas commercial PCR systems have improved heating and cooling rates to reduce amplification time, they are still relatively time-consuming (typically requiring an hour or more per amplification). This can be attributed to the larger thermal capacitance of a system that requires uniformly heating 96- or 384-well plastic PCR plates and reaction volumes of several tens of microliters per well.

Because fast/ultrafast PCR is highly desirable for applications such as timely diagnosis of infectious diseases, cardiac diseases, cancer, neurological disorder diseases, and rapid biowarfare and pathogen identification at the point-of-care (POC) level, many academic and industrial groups have worked on improving PCR systems,[9–15] One commercial PCR system (LightCycler® 2.0, Roche Diagnostics USA, Indianapolis, IN, USA) using air heating/cooling and capillary tubes can perform 30 thermal cycles in 10–60 min, depending on sample volume.[10] However, this system is not suitable for POC testing due to its high power consumption (800 W maximum) and heavy weight (approximately 22 kg). For POC diagnostics for global health care in resource-limited environments, such as in developing countries, a fast/ultrafast PCR system should be portable, robust, simple, easy to use and characterized by low power consumption through miniaturization and integration.

To date, microfluidic-based fast/ultrafast PCR systems have been extensively investigated to reduce amplification time by decreasing sample sizes as well as by increasing heat transfer rates. Resistive heating with microfabricated thin film heaters is most commonly used to control the temperature in the static microfluidic-based PCR system, in which the PCR runs in the microfluidic chamber.[11,12] However, this method requires a complicated fabrication process to integrate the thin film heater and resistance temperature detection sensor on the chip. In the case of continuous-flow PCR on a chip, the PCR amplification occurs when the reaction samples pass thorough three discrete temperature zones.[13] This method can produce faster thermal cycling for PCR, but requires an external syringe pump for continuous-flow control and lacks the ability to perform multiple reactions at the same time. Another approach includes infrared-mediated non-contact selective heating of water droplets (nanoliter sample volume) for ultrafast thermal cycling

[1]Department of Bioengineering, University of California, Berkeley, CA 94720, USA; [2]Berkeley Sensor and Actuator Center, University of California, Berkeley, CA 94720, USA; [3]Department of Electrical Engineering and Computer Sciences, University of California, Berkeley, CA 94720, USA and [4]Biophysics Graduate Program, University of California, Berkeley, CA 94720, USA
Correspondence: LP Lee, Department of Bioengineering, University of California, Berkeley, CA 94720, USA
E-mail: lplee@berkeley.edu
Received 17 November 2014; revised 21 January 2015; accepted 28 January 2015; accepted article preview online 29 June 2015

using an infrared laser, which harnesses the strong absorbance of water at wavelengths over 1000 nm.[14,15] However, droplet formation from the PCR mixture is a precise process prone to human error, which is a drawback for POC testing.

More recently, efforts have been made to utilize the advantages of plasmonic photothermal heating of gold nanoparticles,[16,17] using pulsed or continuous-wave laser excitation for photothermal therapy of cancer[18,19] and fast PCR,[20] for example. However, this arrangement is not ideal for POC testing, as it requires not only expensive lasers and detection systems but also lacks reliable gold nanoparticles-based sample preparation.

In this paper, we present a novel ultrafast photonic PCR method that combines the use of a thin Au film as a light-to-heat converter and light-emitting diodes (LEDs) as a heat source. The strong light absorption of the thin Au film (65%, 120 nm thick) generates heat due to the plasmonic photothermal light-to-heat conversion by photon–electron–phonon coupling at the thin Au film, followed by heating of the surrounding solution with a maximum temperature of over 150 ℃ within 3 min. Thirty ultrafast thermal cycles (heating rate of 12.79±0.93 ℃ s^{-1} and cooling rate of 6.6±0.29 ℃ s^{-1}) from 55 ℃ (point of annealing) to 95 ℃ (point of denaturation) are accomplished within 5 min. Using this technique, we successfully demonstrate the amplification of λ-DNA. We propose that our PCR system would be ideal for POC diagnostics due to its ultrafast thermal cycling capability, multiplex PCR, low power consumption (in the current set-up, up to approximately 3.5 W), low cost and simple configuration for system level integration. Furthermore, our efficient photonic-based heating procedure could be generally integrated into a variety of devices or procedures, including on-chip thermal lysis and heating for isothermal amplifications.

MATERIALS AND METHODS

Fabrication of the thin Au film deposited poly(methyl methacrylate) (PMMA) PCR wells

The 4-mm-thick PMMA sheets were cut with a VersaLASER VL-200 laser cutting system (Universal Laser System, Inc., Scottsdale, AZ, USA) to make a reaction well with a 4-mm diameter. The 1.5-mm-thick bottom PMMA sheet and top reaction wells were bonded together using thermal bonding performed at 84 ℃ with a pressure of 1.0 t after UV/ozone treatment of the PMMA sheet for 10 min. Thin Au films of different thicknesses were deposited by electron beam evaporation under a base pressure of 2×10^{-7} Torr. The thin Au film was passivated with thin poly(dimethylsiloxane) by dropping 2 μL of poly(dimethylsiloxane) into the well and curing in an oven for 2 h to prevent PCR reaction inhibition by the thin Au film and thermocouple.

Simulation

We used COMSOL Multiphysics software (Ver. 4.3, COMSOL Inc., Burlington, MA, USA) for electromagnetic simulation. The detailed geometry and material properties for the simulation are shown in Supplementary Fig. S1 and Table S1. A thin Au film is placed on a PMMA substrate, and then the Au film was covered with water. Different thicknesses (10, 20, 40, 80 and 120 nm) of thin Au film were applied to the simulation to calculate the absorption of the Au films and subsequent resistive heat generation. The plane wave with an *x*-polarized electric field travels in the positive *z* direction in the coordinate system shown in Supplementary Fig. S1. The permittivity of Au used in this study was referred from Johnson and Christy,[21] and the permittivities of PMMA and water were 3 and 1.77, respectively.

Ultrafast photonic PCR cycles

LEDs (Luxeon® Rebel, Lumileds, San Jose, CA, USA, royal blue with a peak wavelength of 447.5 nm, 890 mW at 700 mA injection current) were used for plasmonic photothermal heating of the thin Au film with a Keithley 2400 source meter. To focus the light from the LEDs, a Carclo 20 mm fiber coupling optic (part number: 10356, Carclo Optics, PA, USA) was employed. The temperature of the solution was monitored and recorded in real time by a type-K insulated thermocouple purchased from OMEGA Engineering (part number, 5SC-TT-K-40-36) for thermal cycling. Temperature cycling using an LED, 80 mm cooling fan, source meter and thermocouple was controlled through the LabVIEW program. A National Instruments 9213 16 channel thermocouple module with high speed mode, auto zero and cold junction compensation was used for accurate temperature acquisition from the type-K thermocouple.

Preparation of the PCR reagent and DNA template

The template λ-DNA and Takara Z-Taq™ DNA polymerase (2.5 U μL^{-1}), 10× Z-Taq Buffer (Mg^{2+} plus, 30 mM) and dNTP Mixture (2.5 mM each) were purchased from Takara Bio Inc. (Otsu-shi, SHG, Japan). Forward primer (5′-CATCGTCTGCCTGTCATGGGCTGTT AAT-3′) and reverse primer (5′-TCGCCAGCTTCAGTTCTCTGGC ATTT-3′) were purchased from Integrated DNA Technologies, Inc. (Coralville, IA, USA). The reaction to amplify a 98-base pair (bp) λ-DNA target with Z-Taq™ DNA polymerase included 0.5 μL Z-Taq DNA polymerase, 5 μL of 10× Z-Taq Buffer, 4 μL of dNTP mixture, 4.5 μL of 10 μM primers (each) and 10 μL of bovine serum albumin (50 μg) and was brought to 50 μL with PCR-grade water. The final concentration of the template λ-DNA was 0.1 ng μL^{-1}. The 10 μL of PCR mixture was placed within Au-coated PMMA PCR wells for photonic PCR and then covered with 30 μL of mineral oil to prevent evaporation during thermal cycling. After amplification, a mixture of 10 μL of PCR product and 10 μL of E-Gel® sample loading buffer (Invitrogen, Thermo Fisher Scientific Inc., Waltham, MA, USA) was loaded onto E-Gel® 2% agarose gels with SYBR Safe™ DNA gel stain (Invitrogen) and run in an E-Gel base (Invitrogen) for 30 min. A 1-Kb DNA ladder was used to confirm the size of product.

RESULTS AND DISCUSSION

Photothermal light-to-heat conversion for PCR

The principle of ultrafast photonic PCR is illustrated in Figure 1a. In considering photon interaction with materials, the absorption of photons is often treated as heat.[22] When the photons from the excitation source reach the surface of the thin Au film, plasmon-assisted strong light absorption can occur. This, in turn, excites electrons near the surface to higher energy states, generating hot electrons within 100 fs.[23,24] These hot electrons can reach a temperature of several thousand degrees Kelvin due to their small electronic heat capacity. They are also capable of rapidly diffusing throughout the thin Au film, creating a uniform distribution of hot electrons. Rapid heating is followed by cooling to equilibrium by energy exchange between the hot electrons and the lattice phonons after 5–10 ps. Thus, overall, when thin Au films are illuminated, a large temperature difference between the hot metal surface and the cooler surrounding solution occurs, resulting in the heating of the surrounding solution in a long time scale over 100 ps. When a light is turned off, the fast cooling of the heated solution can also be achieved by the heat dissipation through the thin Au film with high thermal conductivity of 317 W m^{-1} K^{-1}.[25] A thin Au film deposited on a PMMA well is used as a light-to-heat converter, serving as a source of plasmonic photothermal

doi:10.1038/lsa.2015.53

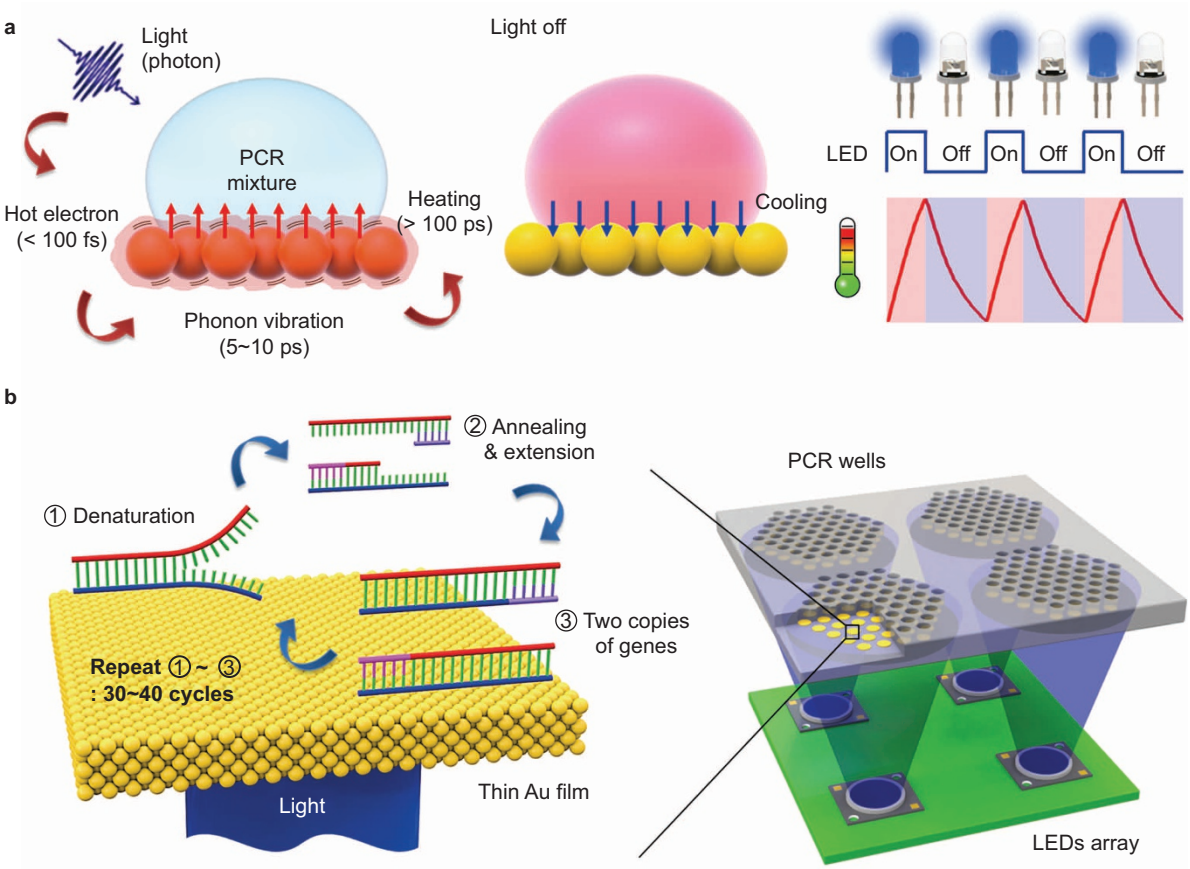

Figure 1 Ultrafast photonic PCR. (**a**) Schematic of the plasmonic photothermal light-to-heat conversion and subsequent heating of the surrounding solution (here, the PCR mixture) through ultrafast photon–electron–phonon couplings. When a light is turned off, fast cooling of heated solution can be achieved by the heat dissipation through the thin Au film. (**b**) Schematics of the ultrafast photonic PCR using a thin gold (Au) film as a light-to-heat converter and excitation light from the LEDs. Thermal cycling, consisting of two or three discrete temperatures for denaturation, annealing and extension, is required for nucleic acid amplification through the PCR. For multiple PCR reactions, each LED could be modulated separately so that there are unique annealing temperatures for each primer design. LED, light-emitting diode; PCR, polymerase chain reaction.

heating for the PCR thermal cycling, as shown in Figure 1b. In addition to driving multiple PCR reactions with single LEDs, multiple well plates integrated with LED arrays could be used for multiplex PCR by modulating each LED to have unique annealing temperatures for the various primer designs. This multiple well LED array PCR thermal cycler configuration would be ideal for multiplex ultrafast PCR for POC diagnostics because it could perform multiple tests at once.

We performed a set of electromagnetic simulations to theoretically characterize the plasmonic photothermal light-to-heat conversion of our Au films. We calculated the electromagnetic field and resistive heat distributions for 10-nm- and 120-nm-thick Au films on a PMMA substrate. As expected from the skin depth, $\delta = \sqrt{\frac{2}{\omega\mu\sigma}}$ where ω is the angular frequency, μ is the permeability and σ is the conductivity; the thickness of the thin Au film determines the amount of light to heat conversion. Upon a normal incidence of a 450 nm wavelength light source, the 10 nm thick Au film transmits an enormous amount of electromagnetic energy (Figure 2a), and the heat conversion energy is saturated along the film depth (Figure 2c). However, the 120-nm thick Au film absorbs most of the incident light (Figure 2b) and subsequently, generates more heat in the Au film by converting light into heat (Figure 2d). Figure 2e shows that an increase in thickness of thin Au film, in the range of 10–120 nm, corresponds to an increase in the optical absorption. A significant increase of the optical absorption below the 540-nm wavelength could be attributed to the plasmonic electron resonance of gold.[26] As a result, the averaged light-to-heat conversion efficiency over the emission wavelength from each LED increases with increasing Au film thickness for three different LEDs, as shown in Figure 2f (see Supplementary Fig. S2). It is noteworthy that the blue LEDs with peak emission wavelength of 450 nm show the highest light-to-heat conversion efficiency using the thin Au film.

LED-driven photonic PCR thermal cycler

The optical absorption spectra of thin Au films with different thicknesses deposited on PMMA substrates are shown in Figure 3a (see Supplementary Fig. S3). Our simulation results can help us determine when the strongest light absorption occurs, as this is critical to maximizing photothermal heating. As the thickness of the thin Au film increases, the optical absorption also increases, showing 65 % absorption at the peak wavelength (450 nm) of the excitation LEDs in the 120-nm-thick Au film. Our photonic PCR thermal cycler uses LEDs as a heating source, PMMA PCR wells deposited with thin Au films, and a lens to focus the excitation light (see Supplementary Fig. S3). The light from the LEDs is continuous-wave and randomly polarized. Therefore, the efficiency of light-to-heat conversion would be lower in this case

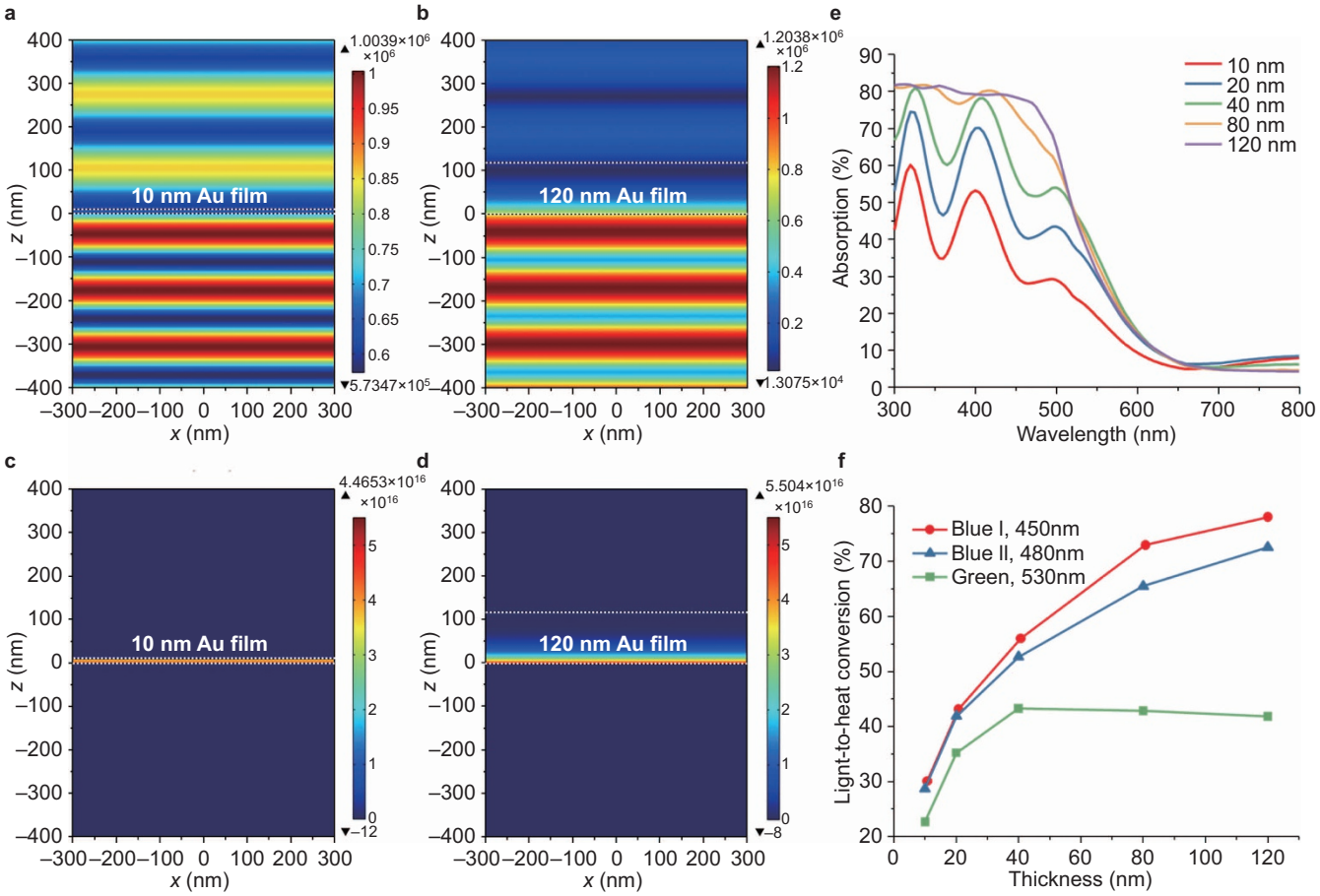

Figure 2 Simulation for heat generation by the thin Au films using electromagnetic radiation. Calculated electromagnetic field distributions for the (**a**) 10 nm- and (**b**) 120-nm-thick Au films on a PMMA substrate. The wavelength of light is 450 nm with a normal incident angle. Corresponding resistive heat distributions for the (**c**) 10-nm- and (**d**) 120-nm-thick Au films on a PMMA substrate. (**e**) Calculated absorption spectra of the thin Au films with different thicknesses. (**f**) Light-to-heat conversion efficiency of the thin Au films averaged over emission wavelength from three different LEDs as a function of Au film thickness. The blue LED with the 450 nm peak wavelength shows the highest averaged light-to-heat conversion efficiency. LED, light-emitting diode; PMMA, poly(methyl methacrylate).

than using a pulsed laser because as electrons are excited to higher energy states, the probability of further excitation decreases. Despite its possibly lower light-to-heat conversion efficiency than a pulsed light source, however, LEDs require minimal power consumption and are extremely low in cost compared with laser sources, making them an ideal PCR heating source for POC testing. The component cost of the instruments for our ultrafast photonic PCR thermal cycle (see Supplementary Fig. S3b) could be less than US$100 including the LEDs, focus lens and driver, if the LabVIEW and data acquisition board for temperature control are integrated into a microcontroller module. The maximum power consumption of an LED is approximately 3.5 W at a 1 A injection current. Figure 3b shows the temperature profiles of 10 μL volumes of solution (here, glycerol was used to show the maximum heating temperatures) upon thin Au films of different thicknesses at a fixed injection current of 500 mA. The maximum temperatures increased as the thickness of the thin Au film increases from 10 nm to 120 nm due to the increasing optical absorption. The photothermal heating of the 120-nm-thick Au film was further characterized as a function of the injection current, as shown in Figure 3c, because the heating rate is determined by the amount of dissipated power (i.e., the injection current of the LEDs). Figure 3d summarizes the temperature of a solution after 3-min heating with Au films of different thickness and varying injection currents (see Supplementary Table S2).

These results clearly indicate that the maximum temperature increases with an increase of Au film thickness to 120 nm and an increase of injection current to 1 A. Complete PCR thermal cycling, consisting of three representative temperatures (94 ℃ for denaturation, 60 ℃ for annealing and 72 ℃ for extension), is demonstrated using an LED-driven photonic PCR thermal cycler, as shown in Figure 3e. To prevent evaporation during thermal cycling, 10 μL of PCR buffer was covered with 30 μL of mineral oil. The averages and standard deviations at each temperature were obtained from the temperature profile, and the results are 94.09±0.17 ℃ at 94 ℃, 59.94±0.13 ℃ at 60 ℃ and 72.02±0.12 ℃ at 72 ℃, respectively, showing excellent temperature accuracy and stability. The initial temperature fluctuation before reaching the setting temperature could be further reduced by optimizing the proportional-integral-derivative controller value in LabVIEW.

Ultrafast thermal cycling and nucleic acid amplification

To determine maximum heating and cooling rates, a thermal cycle was performed whereby the solution (here, 5 μL of PCR mixture covered with 30 μL of mineral oil) temperature was rapidly cycled between

doi:10.1038/lsa.2015.53

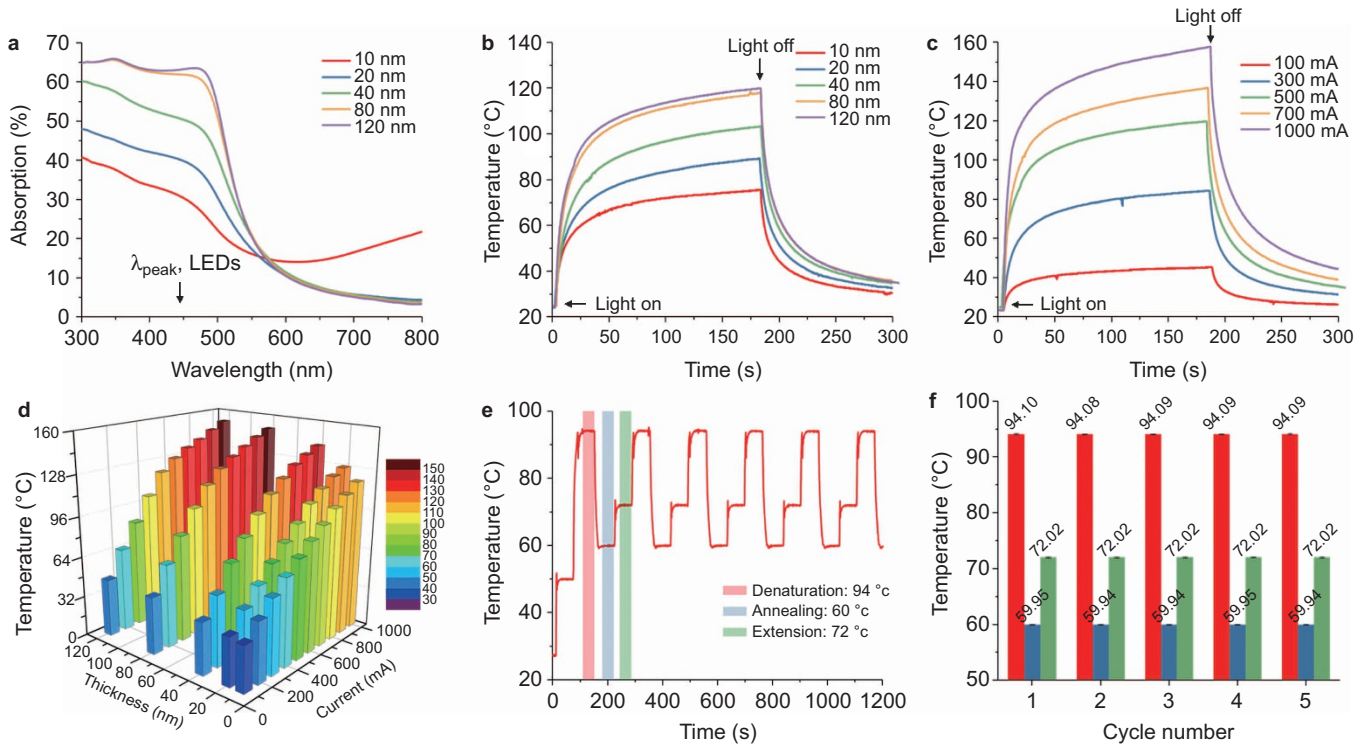

Figure 3 LED-driven photothermal heating of the thin Au films and PCR thermal cycling. (**a**) Absorption spectra of the thin Au films with different thickness. Absorption (%)=100–Transmittance (%)–Reflectance (%). Temperature profiles of liquids (**b**) as a function of Au film thickness with a 500 mA injection current and (**c**) as a function of the injection current of the LEDs using a 120-nm-thick Au film. The blue LED with a 450 nm peak wavelength was used. (**d**) Two-dimensional map showing the distribution of liquid temperatures with different thicknesses of the thin Au film and injection currents of the LEDs after heating for 3 min. (**e**) Demonstration of LED-driven photonic PCR thermal cycling, consisting of three different temperatures; 94 ℃ (denaturation), 60 ℃ (annealing) and 72 ℃ (extension). (**f**) Accurate temperature control and low temperature variation for PCR thermal cycling. The average values with standard deviation at 94 ℃, 60 ℃ and 72 ℃ were 94.09±0.17 ℃, 59.94±0.13 ℃ and 72.02±0.12 ℃, respectively. LED, light-emitting diode; PCR, polymerase chain reaction.

55 ℃ and 95 ℃, mirroring the denaturation (95 ℃) and annealing (55 ℃) temperatures. Figure 4a shows the 30 ultrafast photonic cycles within 5 min. Using the thermal cycling result, heating and cooling rates were calculated by measuring the temperature difference between successive temperature maxima and minima and then dividing by the time interval between them. The average rates and sample standard deviations were obtained as shown in Figure 4b. The average heating and cooling rates obtained are 12.79±0.93 ℃ s^{-1} and 6.6±0.29 ℃ s^{-1}, respectively.

The amplification of λ-DNA was performed to verify our photonic PCR method. After running PCR reactions as shown in Figure 4c, the amplicons were visualized by E-Gel® 2% agarose gels with SYBR Safe™. Lane 1 represents the 1 kb DNA marker, lanes 2 and 3 are the PCR products from ultrafast photonic PCR with different cycle numbers (94 ℃ for 0 s, 62 ℃ for 0 s), and lanes 4 and 5 contain positive controls produced from standard thermal cycling condition (94 ℃ for 1 s, 62 ℃ for 1 s, 60 cycles) by a bench-top thermocycler (Bio-Rad C1000™ Thermal Cycler, Bio-Rad Laboratories Inc., Hercules, CA, USA). Photonic PCR yielded a single 98-bp major band (lanes 2 and 3), indicating that the λ-DNA was successfully amplified using our ultrafast photonic PCR method. The weak band intensity from the PCR product amplified by photonic PCR could be attributed to the lower amplification efficiency compared with a traditional bench-top thermal cycler. Currently, only the thin Au film acts as a two-dimensional photothermal heater, leading to a temperature gradient in the solution and a potentially lower amplification efficiency. This limitation can be improved by utilizing a three-dimensional substrate in the PCR chamber for uniform photothermal heating of the PCR mixture. Amplification time as well as reagent consumption could be further reduced, simultaneously improving the efficiency of the PCR reaction by faster molecular diffusion and uniform solution temperature.

CONCLUSION

In conclusion, we demonstrated a novel ultrafast photonic PCR through plasmonic photothermal heating of thin Au films driven by LEDs. We designed and fabricated a thin Au film-based light-to-heat converter to heat a PCR solution over 150 ℃ by harnessing gold plasmon-assisted high optical absorption. We achieved ultrafast thermal cycling from 55 ℃ (annealing) to 95 ℃ (denaturation) within 5 min for 30 cycles with ultrafast heating (12.79±0.93 ℃ s^{-1}) and cooling (6.6±0.29 ℃ s^{-1}) rates. Nucleic acid (λ-DNA) amplification using our ultrafast photonic PCR thermal cycler was successfully demonstrated. We propose that this simple, robust and low-cost photonic PCR technique with ultrafast thermal cycling capability would be ideal for POC molecular diagnostics, because the photonic PCR technique can meet the 'ASSURED' criteria:[27] (i) **A**ffordable: inexpensive system with a LED and lens; (ii) **S**maller: compact and light PCR system without a heating block; (iii) **S**imple step with disposable PCR chip; (iv) **U**ser-friendly interface with an LED driver and display; (v) **R**apid and robust PCR without environmental stress; (vi) **E**quipment-free: consists of only an LED and

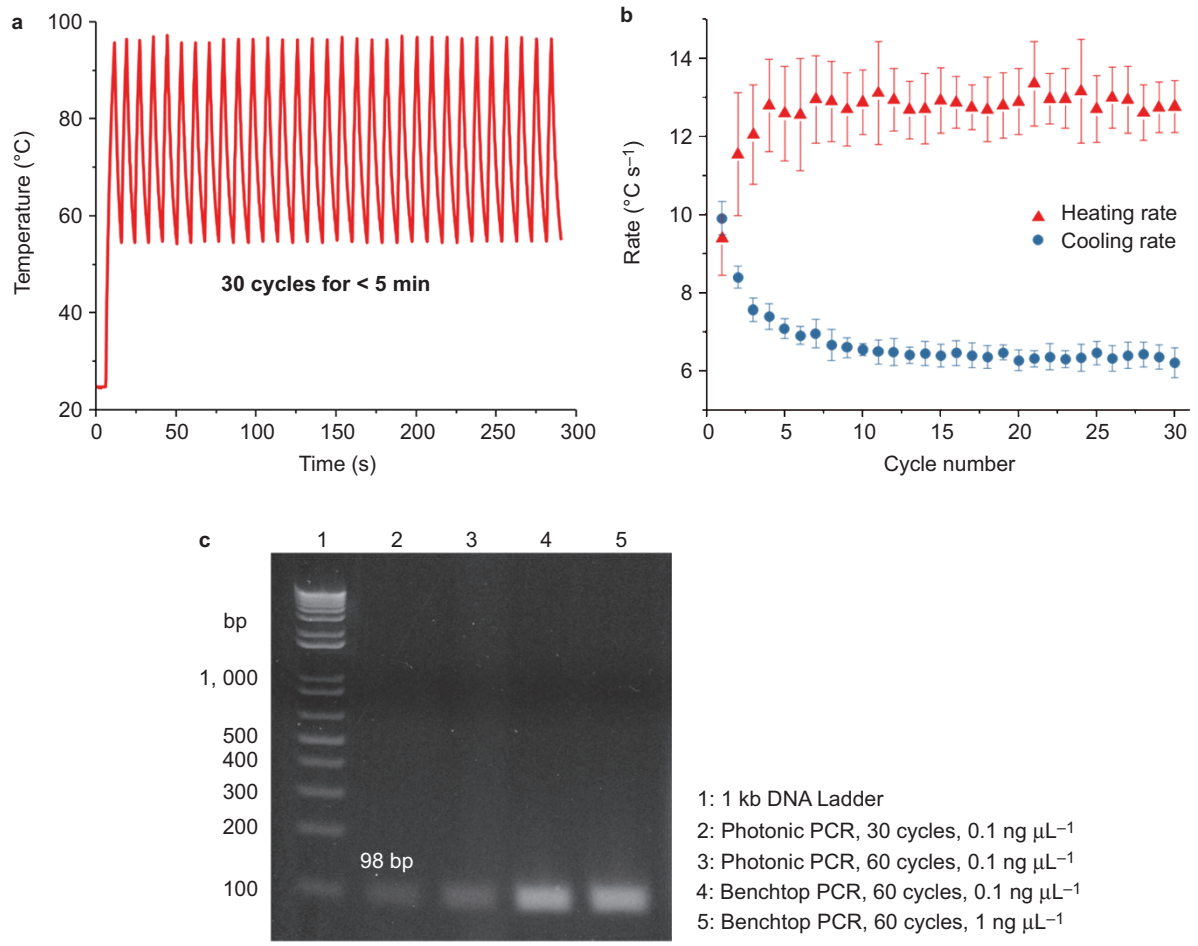

Figure 4 Ultrafast thermal cycling and DNA amplification. (**a**) Representative temperature profiles of 30 ultrafast photonic PCR thermal cycles from 95 ℃ (denaturation) to 55 ℃ (annealing and extension). The 5 μL of PCR buffer was covered with 20 μL of mineral oil to prevent evaporation during thermal cycling. (**b**) Heating and cooling rates obtained from the ultrafast photonic thermal cycling, which were 12.79±0.93 ℃ s^{-1} and 6.6±0.29 ℃ s^{-1}, respectively. (**c**) 2% agarose gel results demonstrating the formation of product from the photonic PCR thermal cycler in comparison with a bench-top thermal cycler using a λ-DNA template. PCR, polymerase chain reaction.

microcontroller modules with a cellphone camera; and (vii) **D**urable in harsh environments and power consumption is low. As the current set-up is based on only one PCR well, future work will focus on integrating more wells and an LED array to allow high-throughput and multiplexed amplification, as well as optimizing the PCR reaction chamber for uniform heating.

ACKNOWLEDGEMENTS

This work was supported in part by a grant from the Bill & Melinda Gates Foundation (Global Health Grant: OPP1028785) and in part by the Global Research Lab Program (2013-050616) through the National Research Foundation of Korea funded by the Ministry of Science, ICT (Information and Communication Technologies) and Future Planning. We thank Karthik R. Prasad and Nusrat J. Molla for helping with the LabVIEW programming for the photonic PCR thermal cycler.

1 Heyries KA, Tropini C, VanInsberghe M, Doolin C, Petriv OI *et al*. Megapixel digital PCR. *Nat Methods* 2011; **8**: 649–651.
2 Ottesen EA, Hong JW, Quake SR, Leadbetter JR. Microfluidic digital PCR enables multigene analysis of individual environmental bacteria. *Science* 2006; **314**: 1464–1467.
3 Barker M. Clever PCR: more genotyping, smaller volumes. *Nat Methods* 2010; **7**: 351–356.
4 Zhang C, Xing D. Miniaturized PCR chips for nucleic acid amplification and analysis: latest advances and future trends. *Nucleic Acids Res* 2007; **35**: 4223–4237.
5 Postollec F, Falentin H, Pavan S, Combrisson J, Sohier D. Recent advances in quantitative PCR (qPCR) applications in food microbiology. *Food Microbiol* 2011; **28**: 848–861.
6 Smith CJ, Osborn AM. Advantages and limitations of quantitative PCR (Q-PCR)-based approaches in microbial ecology. *FEMS Microbiol Ecol* 2009; **67**: 6–20.
7 Girones R, Ferrús MA, Alonso JL, Rodriguez-Manzano J, Calgua B *et al*. Molecular detection of pathogens in water—the pros and cons of molecular techniques. *Water Res* 2010; **44**: 4325–4339.
8 Horsman KM, Bienvenue JM, Blasier KR, Landers JP. Forensic DNA analysis on microfluidic devices: a review. *J Forensic Sci* 2007; **52**: 784–799.
9 Chang CM, Chang WH, Wang CH, Wang JH, Mai JD *et al*. Nucleic acid amplification using microfluidic systems. *Lab Chip* 2013; **13**: 1225.
10 Lyon E, Wittwer CT. LightCycler technology in molecular diagnostics. *J Mol Diagn* 2009; **11**: 93–101.
11 Liu P, Li X, Greenspoon SA, Scherer JR, Mathies RA. Integrated DNA purification, PCR, sample cleanup, and capillary electrophoresis microchip for forensic human identification. *Lab Chip* 2011; **11**: 1041–1048.
12 Lagally ET, Emrich CA, Mathies RA. Fully integrated PCR-capillary electrophoresis microsystem for DNA analysis. *Lab Chip* 2001; **1**: 102–107.
13 Kopp MU, Mello AJ, Manz A. Chemical amplification: continuous-flow PCR on a chip. *Science* 1998; **280**: 1046.
14 Kim H, Vishniakou S, Faris GW. Petri dish PCR: laser-heated reactions in nanoliter droplet arrays. *Lab Chip* 2009; **9**: 1230–1235.

doi:10.1038/lsa.2015.53

15 Terazono H, Hattori A, Takei H, Takeda K, Yasuda K. Development of 1480 nm photothermal high-speed real-time polymerase chain reaction system for rapid nucleotide recognition. *J J Appl Phys* 2008; **47**: 5212–5216.
16 Baffou G, Quidant R. Thermo-plasmonics: using metallic nanostructures as nano-sources of heat. *Laser Photonics Rev* 2013; **7**: 171–187.
17 Webb JA, Bardhan R. Emerging advances in nanomedicine with engineered gold nanostructures. *Nanoscale* 2014; **6**: 2502.
18 Huang X, El-Sayed IH, Qian W, El-Sayed MA. Cancer cell imaging and photothermal therapy in the near-infrared region by using gold nanorods. *J Am Chem Soc* 2006; **128**: 2115–2120.
19 Jaque D, Maestro LM, Rosal B, Haro-Gonzalez P, Benayas A *et al*. Nanoparticles for photothermal therapies. *Nanoscale* 2014; **6**: 9494–9530.
20 Roche PJR, Beitel LK, Khan R, Lumbroso R, Najih M *et al*. Demonstration of a plasmonic thermocycler for the amplification of human androgen receptor DNA. *Analyst* 2012; **137**: 4475–4481.
21 Johnson PB, Christy RW. Optical constants of noble metals. *Phys Rev B* 1972; **6**: 4370–4379.
22 Carey VP, Chen G, Grigoropoulos C, Kaviany M, Majumdar A. A review of heat transfer physics. *Nanoscale Microscale Thermophys Eng* 2008; **12**: 1–60.
23 Inouye H, Tanaka K. Ultrafast dynamics of nonequilibrium electrons in a gold nanoparticle system. *Phys Rev B* 1998; **57**: 11334–11340.
24 Clavero C. Plasmon-induced hot-electron generation at nanoparticle/metal-oxide interfaces for photovoltaic and photocatalytic devices. *Nat Photonics* 2014; **8**: 95–103.
25 Bergman TL, Lavine AS, Incropera FP, DeWitt DP. *Fundamentals of Heat and Mass Transfer*. 7th ed. New York: John Wiley & Sons; 2011.
26 Bréchignac C, Houdy P, Lahmani M. *Nanomaterials and Nanochemistry*. Berlin/New York: Springer; 2007. p208–209.
27 Peeling RW, Mabey D. Point-of-care tests for diagnosing infections in the developing world. *Clin Microbiol Infect* 2010; **16**: 1062–1069.

Supplementary information for this article can be found on the *Light: Science & Applications*' website (http://www.nature.com/lsa/).